Chapter 4

Coordinated Effect of PHEVs With DGs on Distribution System

4.1 Introduction

The last chapter addressed the modified current injection Newton-Raphson based load flow method ($MCINR$) with inclusion of different types of EV load model. The proposed load flow algorithm is used in this chapter and subsequent chapters for the purpose of power flow in distribution system. This chapter presents a 24-hour generation scheduling of DGs in conjunction with PHEVs charging/discharging considering the different types of PHEV's and at different penetration levels of the PHEVs. Further, the effectiveness of DGs in conjunction with PHEV under different levels of demand response (DR) is also evaluated.

As of now electric vehicles are connected to a grid for charging the battery. As a technology matures, the electric vehicle can be also used as a distributed resource/storage. Now-a- days different types with different driving range of vehicles are introduced in the market, for this situation, charging/discharging of electric vehicles are to be properly coordinated with renewable DGs. As the number of electric vehicles increase, the energy storage capacity will also increase. Which may help system to meet load demand in the peak hours so that distribution system becomes more reliable. The charging and discharging of vehicles can be coordinated as per requirement using electricity tariff. Demand response basically reflects changes in the pattern of electricity usages in response to change in price of electricity. In the present chapter, price-based programs (i.e, time of us-

age, critical peak pricing, extreme day pricing, and real-time pricing) are used for demand response analysis. The charging and discharging times of electrical vehicles are preferred during 01 : 00 - 06 : 00 hours and 18 : 00 - 24 : 00 hours. Thus, according to the demand responsiveness of vehicles, the vehicles can be schedule to charge/discharge at prescribed times with consideration of uncertainties in the charging/discharging characteristics of PHEV's.

In this chapter, a base case of distribution system without PHEVs and DGs has been studied to evaluate system performance characteristics. Further, effect of introduction of PHEVs has been investigated in terms of system operating cost, losses, voltage profile, and load flattening. Introduction of DGs has been investigated by simulating different penetration level of PHEVs along with different demand response (DR) levels. The 24-hour DG scheduling is carried out to optimize the system cost, which is function of charging/discharging cost, losses, and cost of DGs power. A Differential Evolution (DE) search algorithm is used to optimize single objective weighted fitness function. 38-Bus test system is used for demonstrate the effects of coordinated chaging/discharging under different demand response levels.

4.2 Problem Formulation

Three types of energy sources are used in this chapter. These are CPG, DGs and V2G connected vehicles. In this section, we describe the mathematical formulation for optimizing the cost (of CPG, DG and PHEV) and losses and voltage deviation of the network. The time step is taken one hour in throughout the problem formulation and any changes in power consumed/produced by PHEVs, and DGs behavior with in hour is neglected.

4.2.1 Objective function

$$Min.F\{(f_1, f_2, f_3)\}.$$

$$f_1 = F_{CPG} + F_{DGs} + F_{PHEVs}. \tag{4.1}$$

$$F_{CPG} = \sum_{h=1}^{24} E_{CPG}(h) C_c(h) \times 1Hour, \tag{4.2}$$

similarly,

$$F_{DGs} = \sum_{d=1}^{N_{DGs}} \sum_{h=1}^{24} E_{DGs}(d,h) C_{DGs}(d,h) \times 1Hour, \tag{4.3}$$

$$F_{PHEVs} = \sum_{e=1}^{N_{PHEVs}} \sum_{h=1}^{24} [E^{PHEV}_{Discharge}(e,h) C_d(h) \times 1Hour - E^{PHEV}_{Charge}(e,h) C_c(h) \times 1Hour]. \tag{4.4}$$

Equation (4.4) has two terms. The first term represent the condition when consumer gets paid for discharging PHEV into the grid. whereas, the second term with negative sign indicates the cost of electricity that consumer pays when charging the PHEV.

Active power loss during 24 hour is obtained as,

$$f_2 = \sum_{h=1}^{24} \sum_{k \in s^i} \sum_{i=1}^{N_B} 0.5 r_{ik} \frac{|V_B(i,h) - V_B(k,h)|^2}{|z_{ik}|^2}, \tag{4.5}$$

and the voltage deviation is expressed as,

$$f_3 = \sum_{i=1}^{N_B} \sum_{h=1}^{24} |V_B(i,h) - 1.00|. \tag{4.6}$$

f_1, f_2 and f_3 are the three functions forming the objective function. It can be seen that, the fitness functions f_1 can become negative depending on the variable values, hence, to avoid the function going negative the objective function is kept as follows,

$$F = min\{(f_1, f_2, f_3)\} = w_1 f_1^2 + w_2 f_2^2 + w_3 f_3^2. \tag{4.7}$$

Where, $w_1 = 0.6$, $w_2 = 0.25$ and $w_3 = 0.15$ [121] Thus, the problem is to determine the optimal values of $E_{DGs}(d,h)$, $E^{PHEV}_{Discharge}(e,h)$ for the given pattern of $C_c(h)$, $C_{DGs}(d,h)$, and $C_d(h)$.

4.2.2 Constraints

There are many condition/requirements which should be satisfied during a normal operating condition of the grid. In this problem, following are the constraints of the problem.

Power balance constraints

The power consumed at each bus is equal to the sum of load power, power required for PHEV charging and losses. The power is generated at buses by connected DGs, CPG and V2G. The load and generation demand should be matched at all times.

Thus, power balance is represented by the following equations.

$$\sum_{h=1}^{24} P_{loss}(h) = \sum_{d=1}^{N_{DG}} \sum_{h=1}^{24} E_{DGs}(d,h) + \sum_{h=1}^{24} E_{CPG}(h) + \sum_{e=1}^{N_{PHEV}} \sum_{h=1}^{24} E_{Discharge}^{PHEV}(e,h) - \sum_{i=1}^{N_B} \sum_{h=1}^{24} P_{load}(i,h) - \sum_{e=1}^{N_{PHEV}} \sum_{h=1}^{24} E_{Charge}^{PHEV}(e,h), \tag{4.8}$$

where,

$$P_{loss}(h) = \sum_{k \in s^i} \sum_{i=1}^{N_B} 0.5 \frac{r_{ik} |V_B(i,h) - V_B(k,h)|^2}{|z_{ik}|^2}. \tag{4.9}$$

Similarly, the reactive power is also to be balanced at each bus. But here we assume that PHEV does not consume or produce reactive power during charging/discharging to the grid. Thus,

$$\sum_{h=1}^{24} Q_{loss}(h) = \sum_{d=1}^{N_{DG}} \sum_{h=1}^{24} Q_{DG}(d,h) + \sum_{h=1}^{24} Q_{CPG}(h) - \sum_{i=1}^{N_B} \sum_{h=1}^{24} Q_{load}(i,h). \tag{4.10}$$

where,

$$Q_{loss}(h) = \sum_{k \in s^i} \sum_{i=1}^{N_B} 0.5 \frac{x_{ik} |V_B(i,h) - V_B(k,h)|^2}{|z_{ik}|^2}. \tag{4.11}$$

DG capacity constraint

This constraint represent the maximum allowable power which can be injected into the grid at any time by a particular dispatchable DG.

$$E_{DG}(d,h) \leq E_{DG-Max}(d,h). \tag{4.12}$$

Number of DGs

The maximum number of DGs that can be installed is taken as ten, which can be scheduled to optimize the problem. All the DGs are not active throughout, it varies according to the availability of DG.

$$\sum_{d} N_{DG_d} \leq 10. \tag{4.13}$$

PHEV energy balance constraints

In this limitation, the systematic energy balance must be validated for each PHEV during different activities such as charging, discharging and the previously stored energy in the

battery.

$$\sum_{h=1}^{24} E_{store}^{PHEV}(e,h) \leq P_{Bat-Cap} \tag{4.14}$$

$$E_{store}^{PHEV}(e,h) = E_{store}^{PHEV}(e,h-i) + E_{Charge}^{PHEV}(e,h) - E_{used}^{PHEV}(e,h) - E_{Discharge}^{PHEV}(e,h).$$

The charging and discharging phenomena can not happen simultaneously. So that this limitation should also be satisfied

$$\begin{aligned} E_{Charge}^{PHEV}(e,h) &\leq P_{charge-max}(i) \times X \\ E_{Discharge}^{PHEV}(e,h) &\leq P_{Discharge-max}(i) \times Y \end{aligned} \tag{4.15}$$

Where X, Y are binary (0,1). so, that $X \times Y = 0$ which means the vehicle can be charge or discharge up to its maximum capacity in one-by-one fashion.

4.3 Problem Solving Methodology

4.3.1 Power flow analysis

The modified Current Injection Newton-Raphson based load flow Method (MCINR) is used to perform power flow analysis. To validate efficacy and robustness of proposed load flow algorithm $MCINR$ is tested on both the unbalanced radial system (18-, 84- and 140-bus) and meshed distribution test systems (24-, 118- and 300-bus) in previous chapter. It is observed that the convergence characteristic in terms of maximum power mismatch is better in case of modified current injection Newton-Raphson ($MCINR$) as compared to existing current injection based load flow algorithm. In this method $2n$ set of current injection equation are written in rectangular coordinates and the jacobian matrix ($2n \times 2n$) has the same structure as nodal admittance matrix [158]. The program for $MCINR$ power flow was coded in MATLAB.

4.3.2 Optimization methodology

Differential Evolution (DE) is a simple and robust stochastic search algorithm for global optimization [159]. The method requires only three control parameters: Population size (N_P), Mutation scale factor (F) and Crossover rate (C_r). The parameters C_r and F decides how efficiently the DE algorithm explores and exploits the solution search space. N_p is the population at an iteration. N_p decides how many solution points the algorithm

parallely handles. A large values of N_p increases the time taken complete an iteration and vice versa. The popularity of DE has increased among researcher because it is easy to use and its effectiveness over other methods is already demonstrated by many researchers in different areas [160], [161] and [162].

There are four basic stages of DE, which algorithm performs: Initialization, Mutation, Crossover and Selection. The basic procedure of DE is presented in Fig. 4.1.

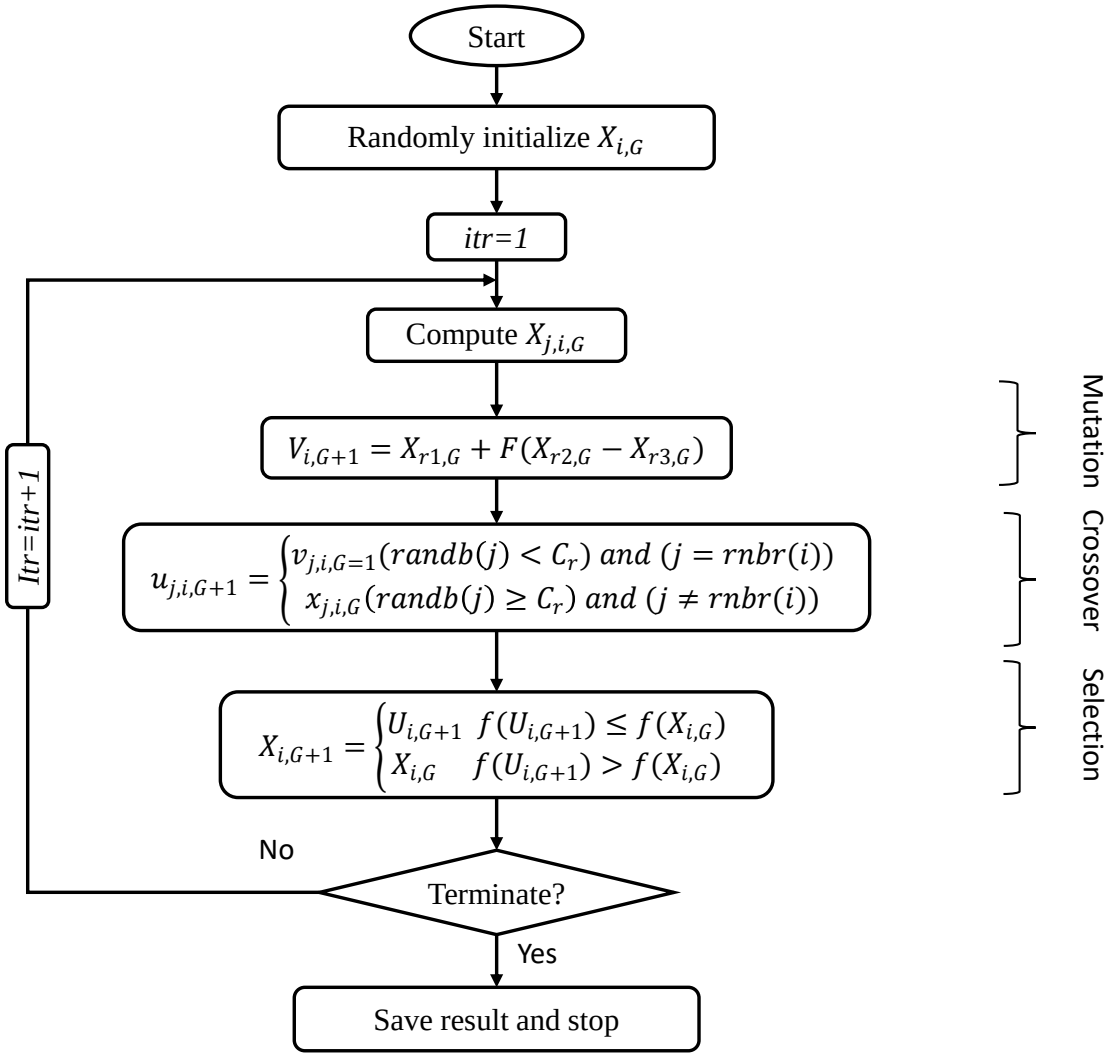

Figure 4.1: Flow chart of Differential Evolution

Initialization

In initialization stage, the control parameters N_p, F and C_r are initialized. The initial population generated should cover the entire search space. The population is generated from uniformly distributed random numbers of solution space. These random variables are within the prescribed lower and upper bounds. The succeeding generation in DE is denoted by Generation number (G) $G = 0, 1, 2, ...G_{max}$. so, the i^{th} individuals for present generation is denoted by the following equation.

$$X_{i,G} = [x_{1,i,G}, x_{2,i,G}, x_{3,i,G}, , , , , , x_{D,i,G}], \tag{4.16}$$

where D is the dimension of the problem and $i = 1, 2, 3....N_P$.

Similarly, the initial value of the j^{th} index of the i^{th} individual of population can be generated by

$$x_{j,i,0} = x_{j,i\ min} + rand[0, 1].(x_{j,i\ max} - x_{j,i\ min}), \tag{4.17}$$

where $rand[0, 1]$ is a uniformly distributed random number variable within the range $\in [0, 1]$.

After initialization, all the individuals are updated in an optimization iteration cycle which is repeated until the terminated condition is met. The updated population forms the new generation.

Mutation

The mutation operation is performed by mutation. The mutation scheme is carried out by randomly choosing three mutually exclusive individuals ($X_{r1,G}$, $X_{r2,G}$ and $X_{r3,G}$) from current population for each individual. Then mutuant individual $V_{i,G+1}$ is obtained by using the following process.

$$V_{i,G+1} = X_{r1,G} + F(X_{r2,G} - X_{r3,G}), \tag{4.18}$$

where $X_{r1,G}$ is called target vector and $X_{r2,G}$, $X_{r3,G}$ are called base vectors. Random indices $r_1, r_2, r_3 \in \{1, 2, 3....N_p\}$ are mutually different integers and they are also chosen to be different from running indexes i, so $N_p \geq 4$. Mutation scale factor $F \geq 0$ is a real and constant factor $\in [0.5, 0.9]$ which controls amplification of the differential variation $(X_{r2,G} - X_{r3,G})$.

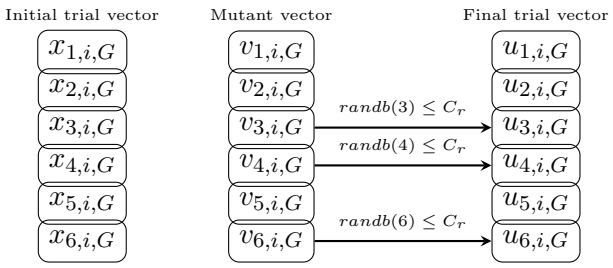

Figure 4.2: Illustration of crossover process for D=6

Crossover

For diversity enhancement of current population, after mutation scheme, DE performs crossover operation. In DE, generally binomial crossover strategy is used to generate trial vector. A new trial vector $U_{i,G} = [u_{1,i,G}, u_{2,i,G}, u_{3,i,G}....., u_{D,i,G}]$, is generated by crossover of mutant vector $V_{i,G+1}$ and a target vector $X_{i,G}$. The generation of trial vector is controlled by crossover rate C_r. The elements, $u_{j,i,G+1}$, of the trial vector, $U_{i,G+1}$, are obtained from mutant vector, $V_{i,G+1}$, and the target vector, $X_{i,G}$, through following crossover process.

$$u_{j,i,G+1} = \begin{cases} v_{j,i,G+1} & (randb(j) \leq C_r) \; and \; (j = rnbr(i)) \\ x_{j,i,G} & (randb(j) > C_r) \; and \; (j \neq rnbr(i)) \end{cases} \tag{4.19}$$

where, $randb(j) \in [0, 1]$ is the j^{th} evaluation of a uniform random number generator, $C_r \in [0, 1]$ is the crossover rate, $rnbr(i)$ is a randomly chosen index $\in$ 1,2,....D which ensures that $u_{j,i,G+1}$ gets at least one parameter from $v_{j,i,G+1}$. Fig 4.2 shows the schematic of crossover procedure in which the target vector $X_{i,G}$ and the mutant vector $V_{i,G+1}$ for D=6 are shown. Trial vector $U_{i,G+1}$ is initialized to $X_{i,G}$ and as the crossover process is performed, the elements of mutant vector $V_{i,G+1}$ replace the elements of $X_{i,G}$.

Selection

Selection compares the vector $U_{i,G+1}$ with vector $X_{i,G}$ in terms of their fitness values to update the location of i^{th} individual in current population to the next iteration($G = G+1$).

$$X_{i,G+1} = \begin{cases} U_{i,G+1} & f(U_{i,G+1}) \leq f(X_{i,G}) \\ X_{i,G} & f(U_{i,G+1}) > f(X_{i,G}), \end{cases} \tag{4.20}$$

where $f(X)$ is the objective function to be minimized. If the new trial vector yields an equal or lower value of the objective function, it replaces the corresponding target vector

in generation. In the present work the optimization was performed to determine the (1) Optimal power generation for the 10 DGs units at the specified buses. (2) Optimal power discharging for PHEV at 8 residential buses. Thus, altogether there are 18 decision variables whose optimal values are to be determined.

For different study cases the number of variables ware adjusted accordingly for eg. when system with DG case was studied, 10 variables were considered, when both DG and PHEV were studied, 18 variables were taken.

The other parameters were fixed as follows: $F = 0.7$, $C_r = 0.9$ and $N_p = 80$.

4.4 Description of Test System

The 38-bus distribution system network [163] shown in Fig.3.2 has been considered for this study. The detailed specification with bus-wise load type and MVA capacity of the test system can be found in [163]. The system data and types of customers are listed in Appendix I. The distribution system is energized through CPG which is connected at bus-1. For 38-bus system, hourly average load distribution of ref. [2] has been considered as shown in Fig. 4.3.

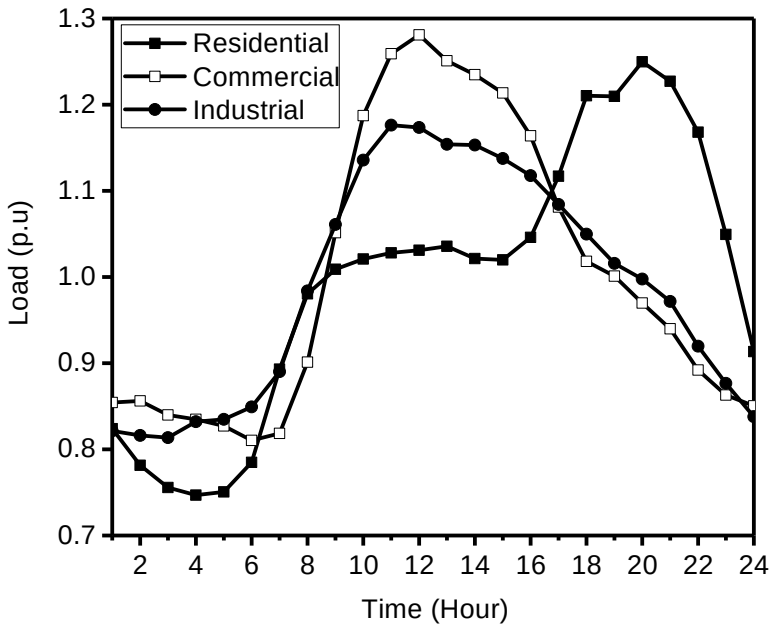

Figure 4.3: Average load demand

Algorithm 3: DE algorithm for solving problem

Generate uniformly distributed random population $X_{i,G}$;
While (NFC $< MAX_{NFC}$) &&; (BFV $>$ VTR)
{
for $(i = 0;\ i < N_P;\ i++)$
{
Select three individual $X_{r1,G}$,$X_{r2,G}$ and $X_{r3,G}$ from current population, where $i \neq r_1 \neq r_2 \neq r_3$;
$V_{i,G+1} = X_{r1,G} + F(X_{r2,G} - X_{r3,G})$;
for$(j = 0; j \leq D; j++)$
{
if $(rand(0,1) < C_r)$
$u_{j,i,G+1} = v_{j,i,G+1}$;
else
$u_{j,i,G+1} = x_{j,i,G}$;
}
Evaluate $U_{i,G+1}$;
$NFC = NFC + 1$;
if $(f(U_{i,G+1}) \leq f(X_{i,G})$;
$X_{i,G+1} = (U_{i,G+1})$;
else
$X_{i,G+1} = X_{i,G}$;
}
BFV=Min(F);
}

The vehicle characteristics adopted in this chapter as per design perspective and generation of stochastic simulation of PHEV load considering the uncertainties related to driving pattern is discussed in chapter 2. Stochastic Model of PHEVs load based on demand response with variation in penetration levels developed in subsection 2.5 is used in this chapter. A total of 100 PHEVs and 10 DGs are considered in this study.

In this study, for the above-mentioned 38-bus system, selection of candidate buses for the DGs integration are determined on the basis of minimization of energy losses in the system. The detailed characteristics of DGs including the type of DGs and the hourly availability are given in Appendix II as reported in [164]. The selection of candidate buses has been performed for all dispatchable DGs in 38-bus system using a Mixed Integer Non-Linear Programming (MINLP) approach as given in Appendix III .

The tariff related to electricity price and the cost paid by DSO to customer for discharging the PHEVs battery into the grid are given in Table 4.1.

Table 4.1: Price of the electrical power produced by the CPGs and discharging price in V2G mode

Hour	1	2	3	4	5	6	7	8	9	10	11	12
Charging Price(€)	0.07	0.06	0.06	0.06	0.06	0.07	0.07	0.08	0.09	0.1	0.1	0.1
Discharging Price (€)	0.06	0.05	0.05	0.05	0.05	0.06	0.06	0.07	0.1	0.11	0.11	0.11
Hour	13	14	15	16	17	18	19	20	21	22	23	24
Charging Price(€)	0.09	0.09	0.1	0.1	0.12	0.13	0.15	0.16	0.16	0.15	0.13	0.1
Discharging Price (€)	0.1	0.1	0.11	0.11	0.13	0.14	0.16	0.17	0.15	0.14	0.12	0.09

4.5 Case Studies: Results and Discussions

Charging and discharging of PHEVs can have both beneficial and adverse effects on the distribution system. The uncertainty in loading pattern due to increased penetration of PHEVs affects the distribution system parameters such as peak load, voltage profile, energy losses and energy cost. The discharging of PHEVs (in V2G mode) during peak loads can be used for saving off the peaks (V2G). The DGs present in the distribution system will have their own effects. It is important to study the effects of DGs in the distribution system with PHEV penetration under different levels of demand response. It

is also important to segregate the effects of DGs and PHEV so that one may be able to understand their individual and combined effects.

Following three cases studies are designed to demonstrated the effects PHEVs and DGs in different DR conditions.

1. Case-I: Base case; In this case it is assumed that there are no PHEVs and DGs. This base case is used to compare the effects of inclusion of PHEVs and DGs. In base case, the following are studied.

   (a) Loading pattern and peak load for residential load.

   (b) Hourly voltage profile and bus-wise voltage profile.

   (c) Energy losses.

   (d) Overall energy cost.

2. Case-II: System with PHEVs; In this case we assume that PHEVs are present and charged and discharged at the residential buses. For the charging and discharging hours already coordinated as described in subsection 2.3.1, the following are studied.

   (a) Loading pattern and peak load for residential load at different penetration levels and the effect of DR.

   (b) Hourly voltage profile and bus-wise voltage profile in presence of PHEVs with different penetration levels and on different DR levels.

   (c) Comparison of energy losses with that of Case-I (Base case) and comparison of energy losses at different DR levels.

   (d) Comparison of energy cost when PHEVs are considered to that of base case.

3. Case-III: System with PHEVs and DGs; In this case the effects of addition of DGs to the system with PHEVs are demonstrated. The following system characteristics are studied.

   (a) Effect of DGs on loading pattern and peak load of system.

   (b) Effect of addition of DGs on hourly voltage profile and bus-wise voltage profile with different penetration levels and on different DR levels.

(c) Effect of addition of DGs on system energy losses and comparison of energy losses at different DR levels,

(d) Effect on the system energy cost.

4.5.1 Case-I: Base case

The base case represents system without PHEV and DGs, i.e only conventional loads are present on the buses. The loading pattern and peak load demand of residential loads are shown in Fig. 3.3. Fig. 3.3 shows that peak loading demand for residential load occurs at $20:00$ hour. Hourly minimum system voltage profile is shown in Fig. 4.4. It is observed that the system voltage is lowest during 12:00 hour. This is due to the peak loadings of industrial and commercial loads during 12:00 hour. The bus-wise voltage profile at a valley hour (04:00 hour) and at peak hour (20:00 hour) is shown in Fig. 4.5. It is observed that bus-wise voltage profile at 20:00 hour goes lower as compare to $04:00$ hour due to peak loading of residential load. The total energy loss for 24 hour is 4.9778 MW and hourly energy loss is shown in Fig. 4.6. The total cost of the power produced by CPG is obtained as € 9578 for 24 hour.

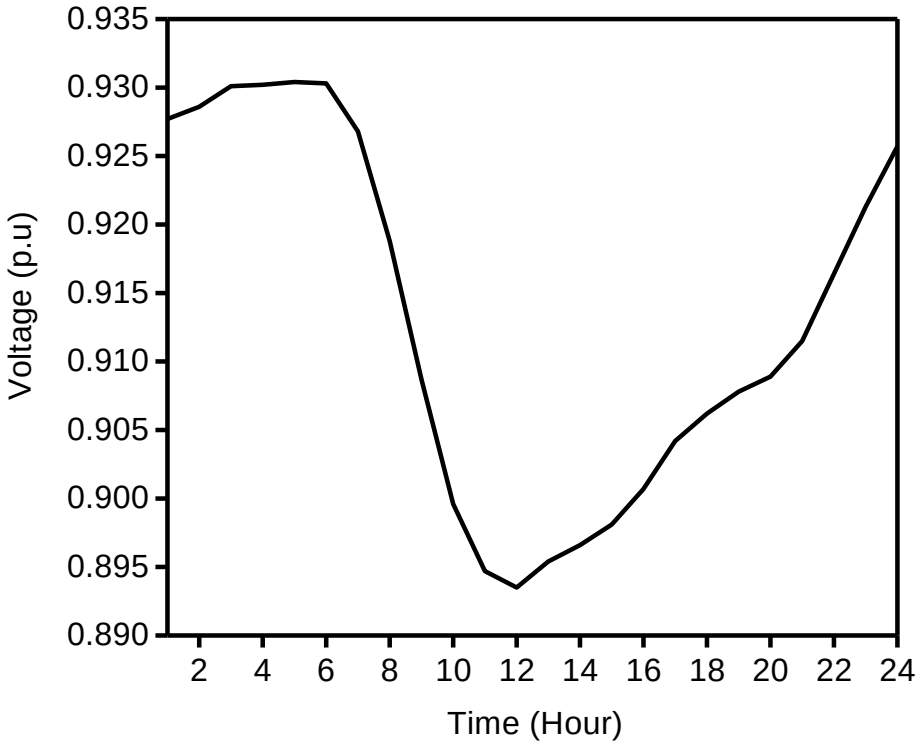

Figure 4.4: Case-I: Hourly minimum voltage

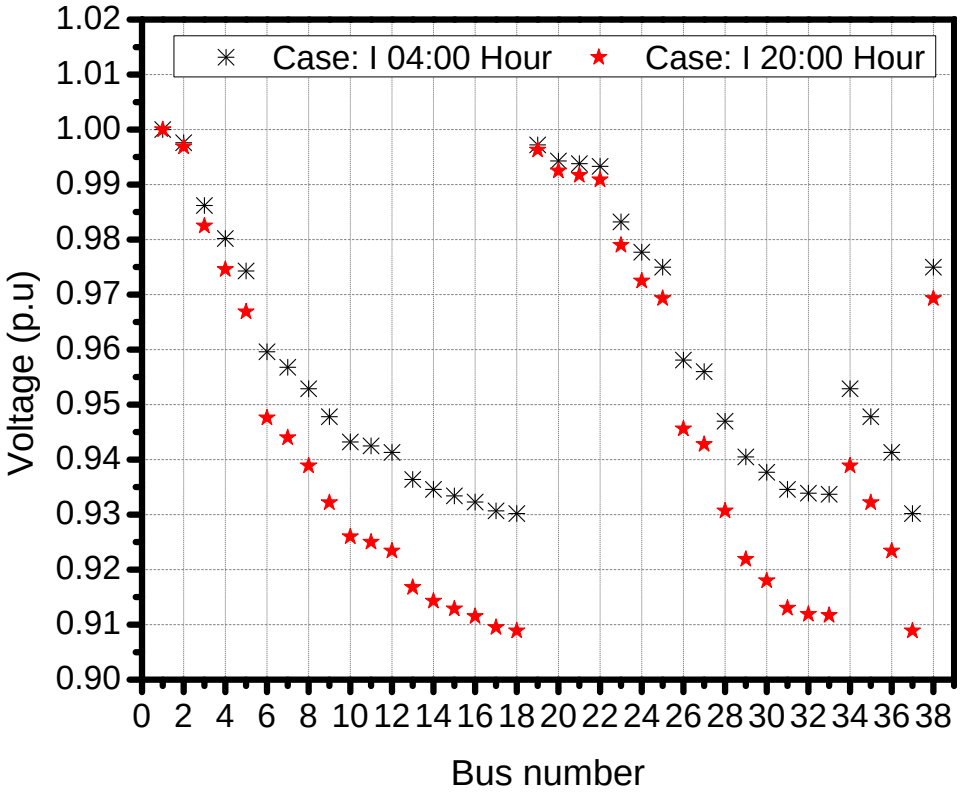

Figure 4.5: Case-I: Voltage profiles during peak (20^{th} hour) and valley load periods (04^{th} hour)

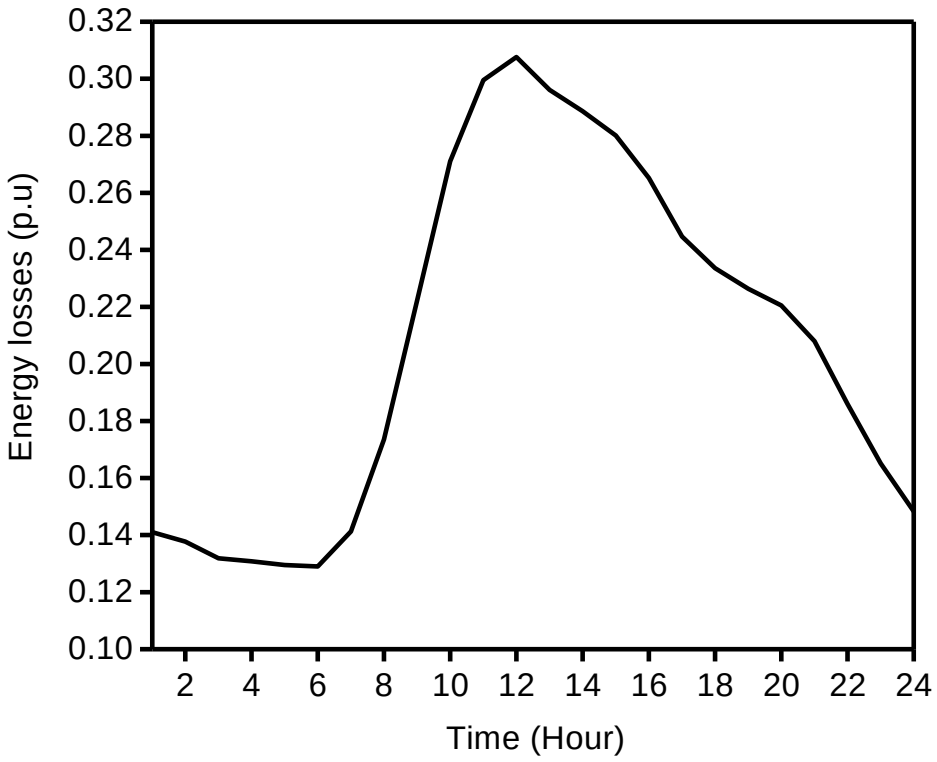

Figure 4.6: Case-I: Hourly energy losses

4.5.2 Case-II: System with PHEV

In this case, three levels of PHEV penetration are considered with three different DR levels. Also the load scenario of the distribution network takes into the account the combined load profile of PHEV and conventional load. However, the PHEVs are considered (both for charging/discharging) on residential buses only. The loading pattern and peak load saving off for residential load is shown in Figs. 4.7 & 4.8. Figs. 4.7 & 4.8 shows the 24-hour load profile for the system without PHEV (base load) and system with PHEV load at penetration levels of 35%, 54% and 62% of vehicles. Figs. 4.7 & 4.8 also shows the peak load shaving for residential load on different levels of DR. The V2G connection

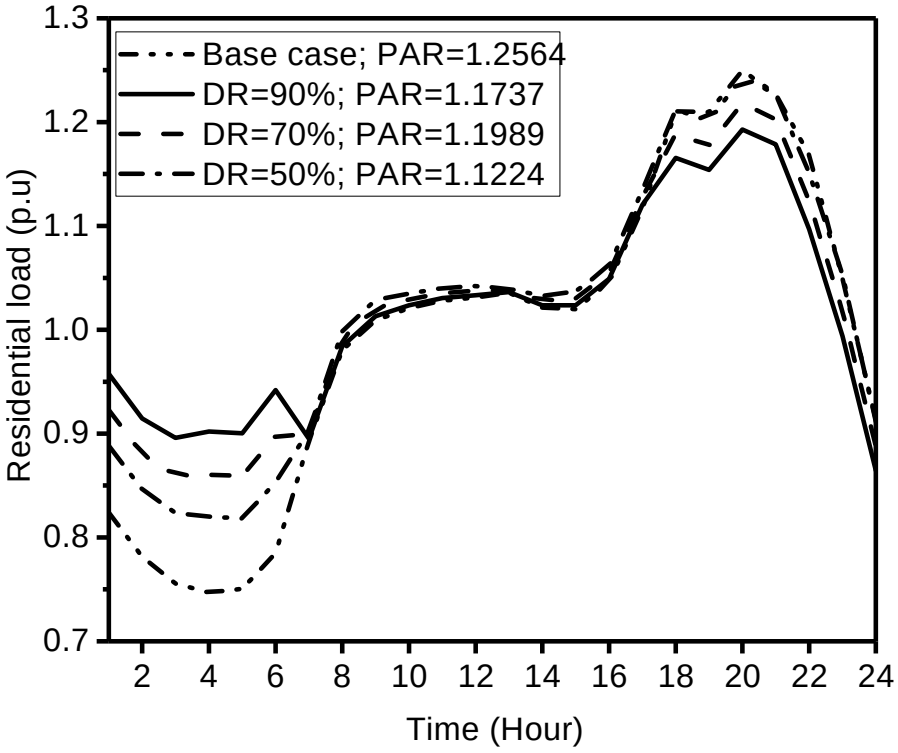

Figure 4.7: Residential load demand at 62% penetration level

of PHEV at higher penetration level leads to increased energy storage capacity in the grid during peak hours that results in reducing the peak load during (18 : 00 - 24 : 00 hour) whereas, during valley hours (1 : 00 - 6 : 00) the load is increased due to charging. As the penetration of PHEVs will increase in future, there is possibility to achieve same or lower PAR compared to no PHEVs in the system.

The hourly minimum system voltage for 24 hour at different penetration levels and

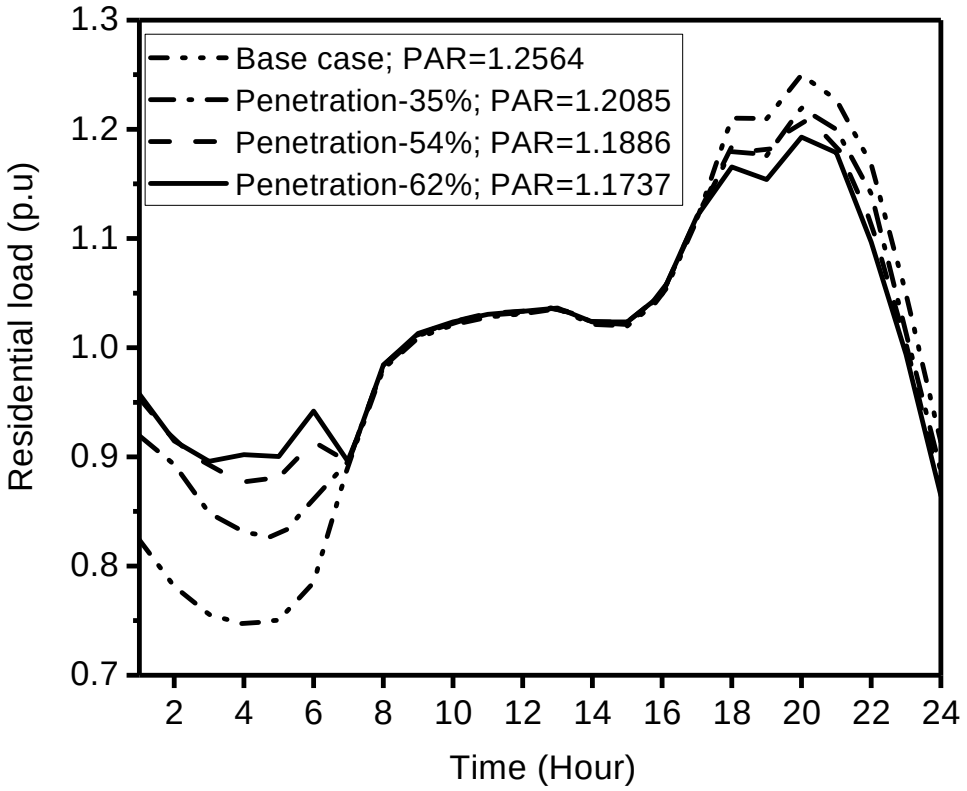

Figure 4.8: Residential load demand at 90% DR

at different DR levels are shown in Figs. 4.9 & 4.10. As far as system voltage profile is concerned, regardless of penetration level, it is observed that there is hardly any improvement in the minimum voltage level during 12:00 hour when compared to the base case. This is due to fact that the V2G and G2V effects are hardly present during these hours. However, as depicted in Figs. 4.9 & 4.10 the voltage levels during G2V mode (1 : 00 - 6 : 00 hour) go lower than the base case values whereas, during V2G mode (18 : 00 - 24 : 00 hour) the voltage profile improves. However, it may be seen that the voltage profiles are not severely affected by PHEV charging/discharging.

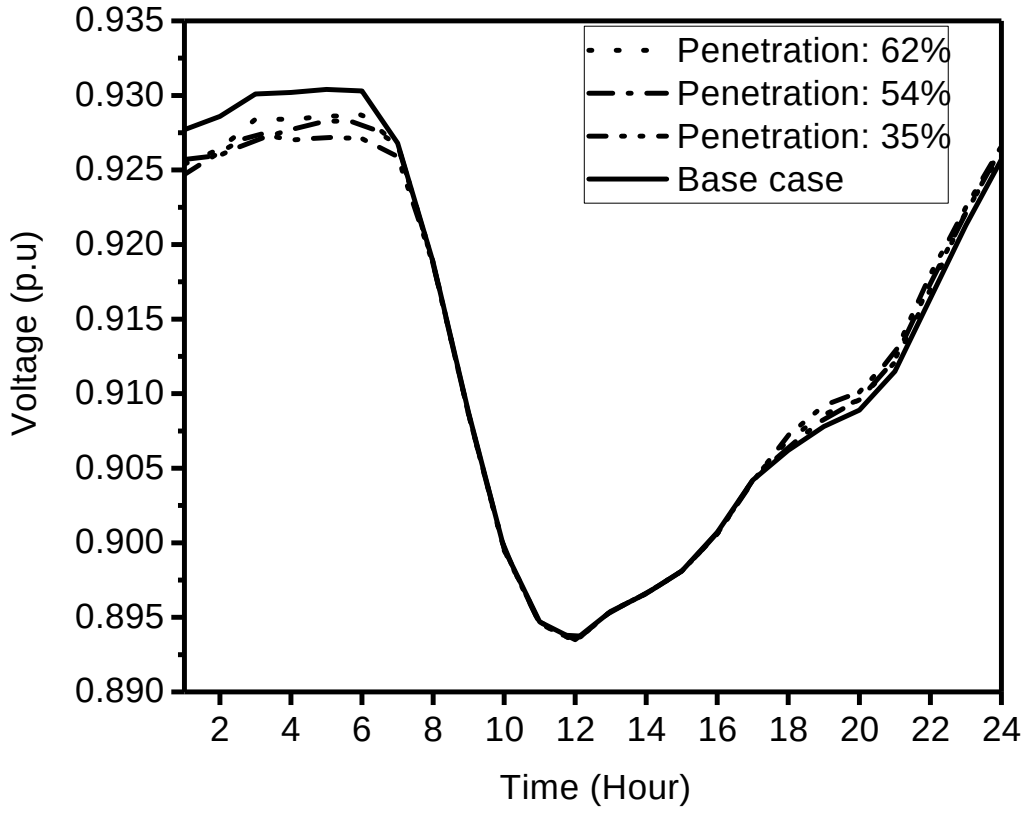

Figure 4.9: Case-II: Hourly Minimum voltage at 62% penetration level

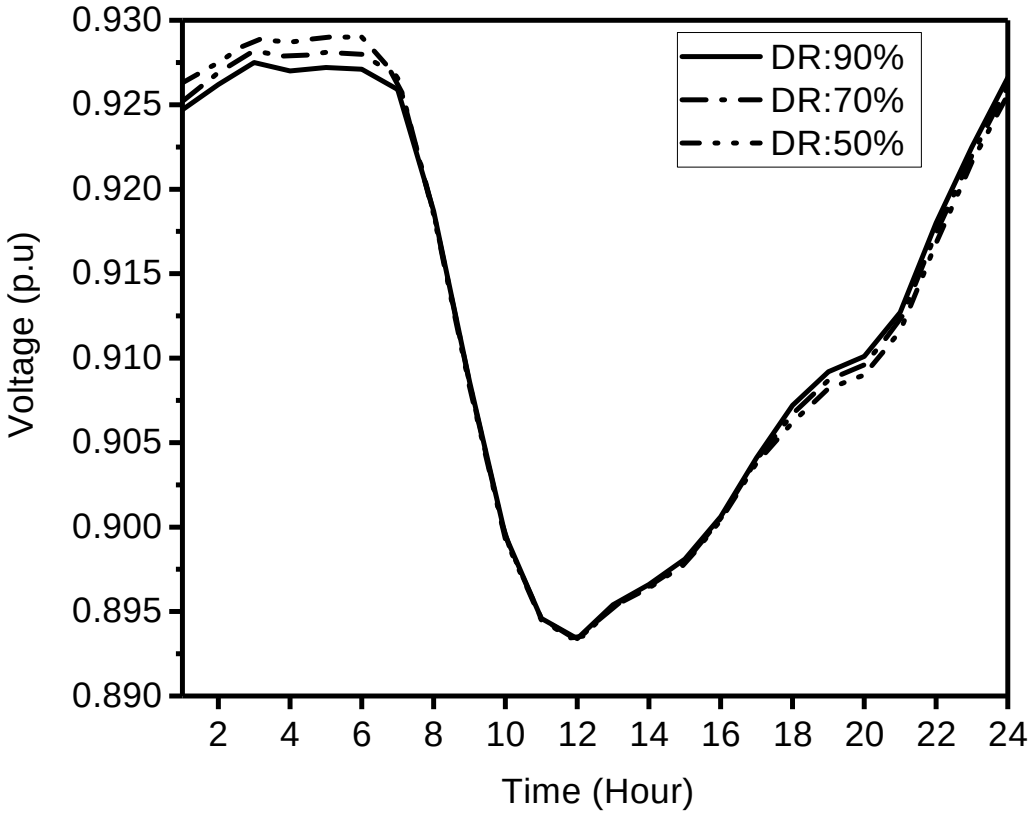

Figure 4.10: Case-II: Hourly Minimum voltage at 90% DR

The bus-wise system voltage profiles for 04 : 00 hour and 20 : 00 hour at 62% penetration level are shown in Fig 4.11. This Figure shows the comparison of bus wise voltage profile for Case-I and Case-II at valley periods (04 : 00 hour) and at peak hour (20 : 00 hour). It is observed that at both periods bus-wise voltage profile gets lower in Case-II, i.e, when PHEVs are incorporated in the distribution system.

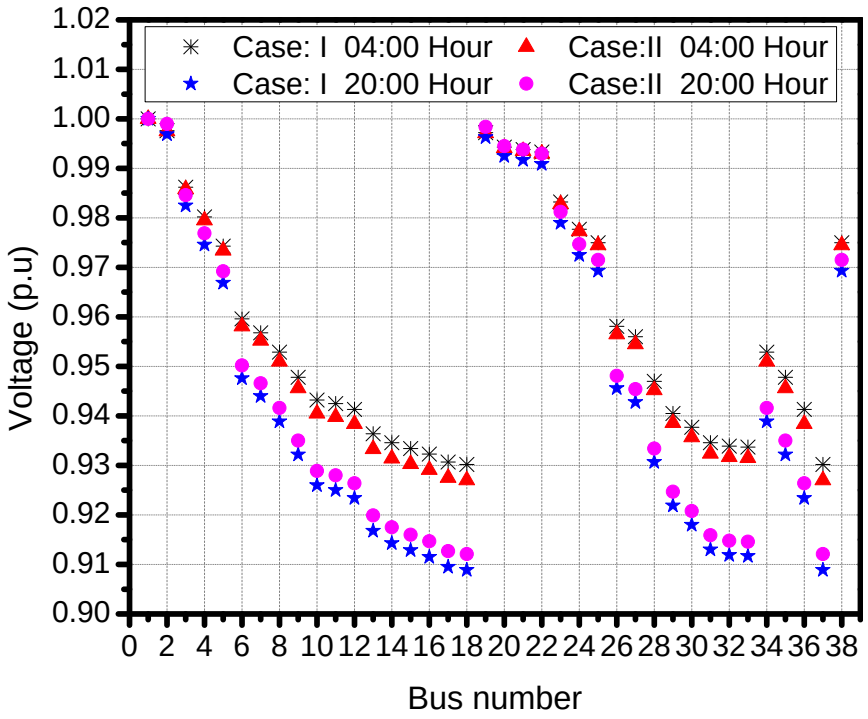

Figure 4.11: Comparison of bus wise-Voltage profiles during peak (20^{th} hour) and valley load periods (04^{th} hour).

The hourly energy losses at different penetration levels and at different DR level of vehicles are shown in Figs. 4.12 & 4.13. The distribution network is analyzed with different penetration levels and it is observed that the total system cost and energy loss decreases as the penetration level goes up. The outcomes of Case-II are summarised in Figs. 4.14 & 4.15. Fig. 4.14 shows the characteristics of system cost versus DR and for different penetration levels. It is observed that the optimal system cost characteristics consistently goes lowers with DR. Thus, it is observed that the DR and penetration levels effects the cost quite significantly. Fig. 4.15 shows the characteristics of energy losses versus DR and for different penetration levels. In the present scenario, it is observed that for penetration level of 62% and at DR of 50% the energy losses are higher than penetration level of 54% at same DR. However, at other levels of DR, the energy losses consistently lowers with penetration level. The optimal system cost shows quite consistent

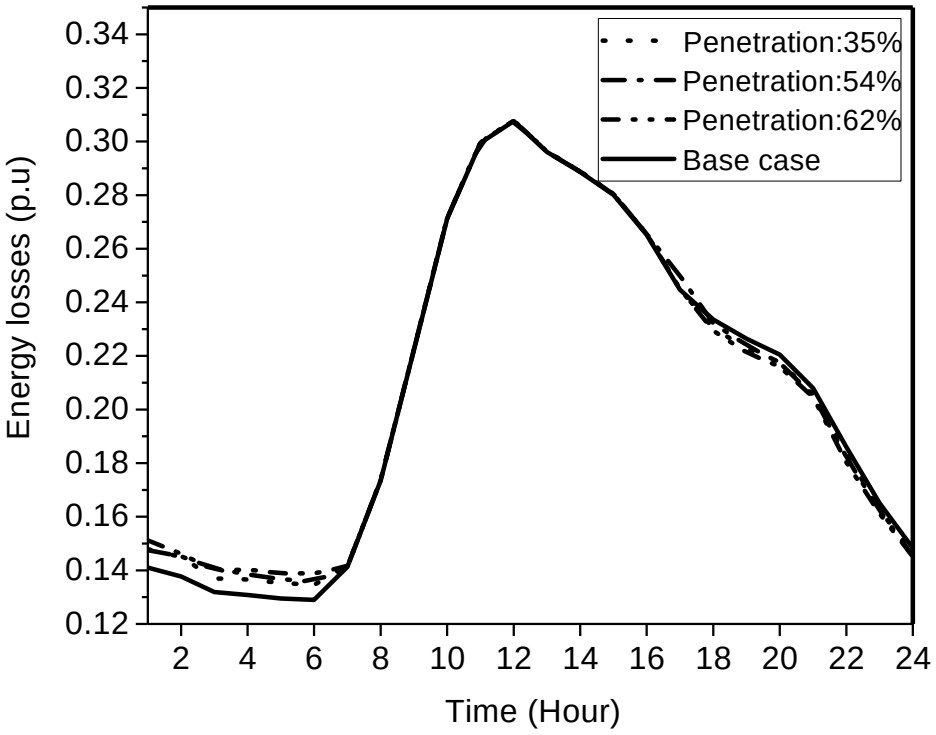

Figure 4.12: Case-II: Hourly energy losses at 90% DR.

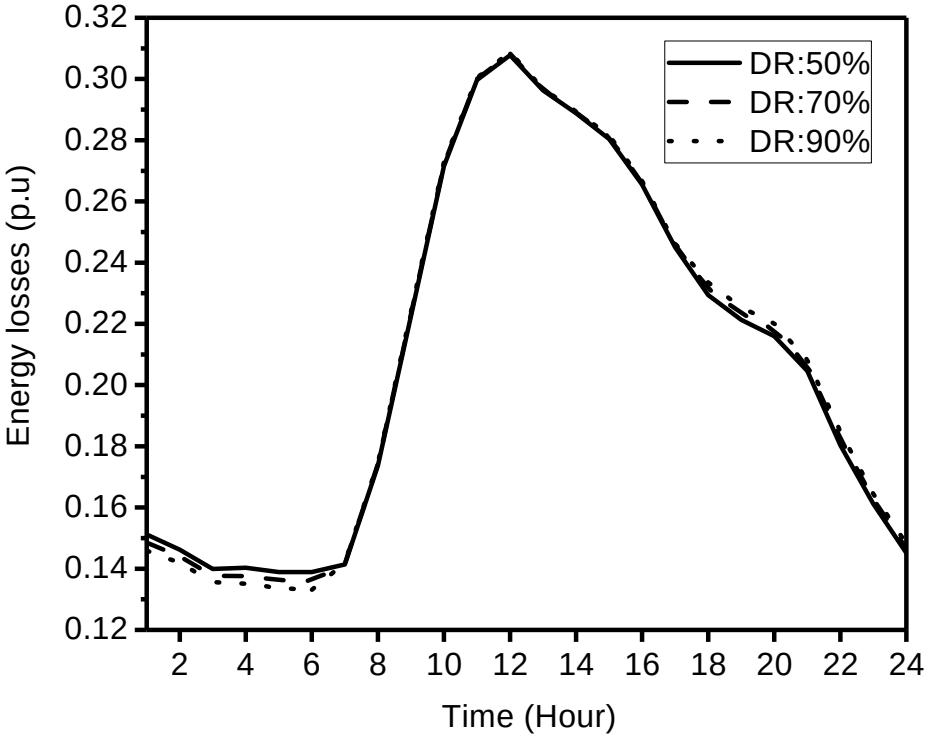

Figure 4.13: Comparison of energy losses without DGs based on DR at 62% level.

effects with respect to penetration levels.

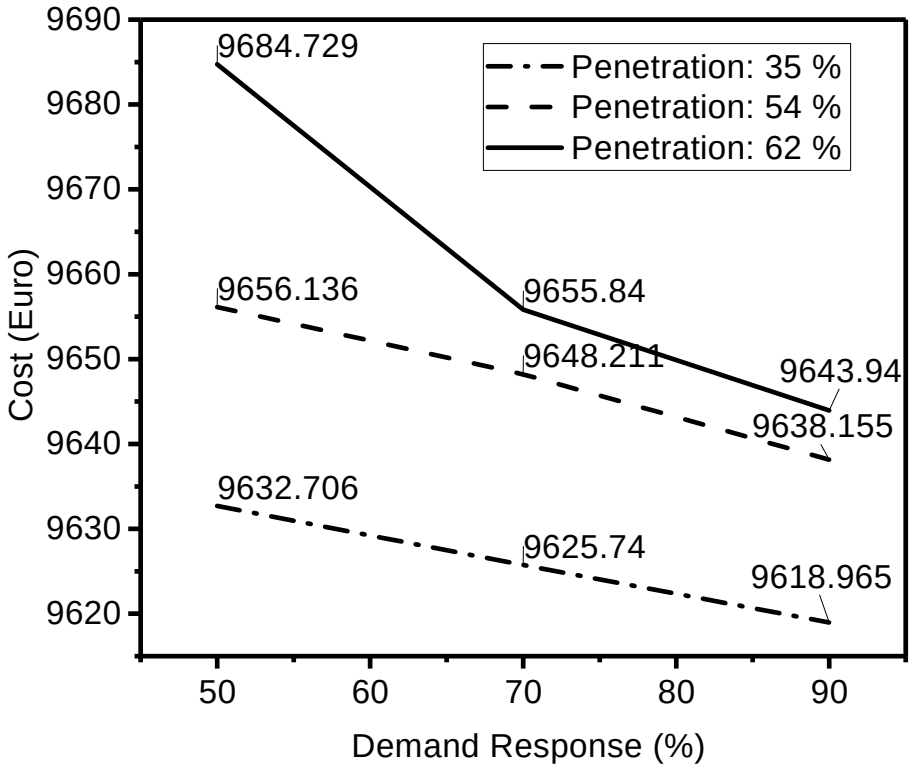

Figure 4.14: Case-II System cost.

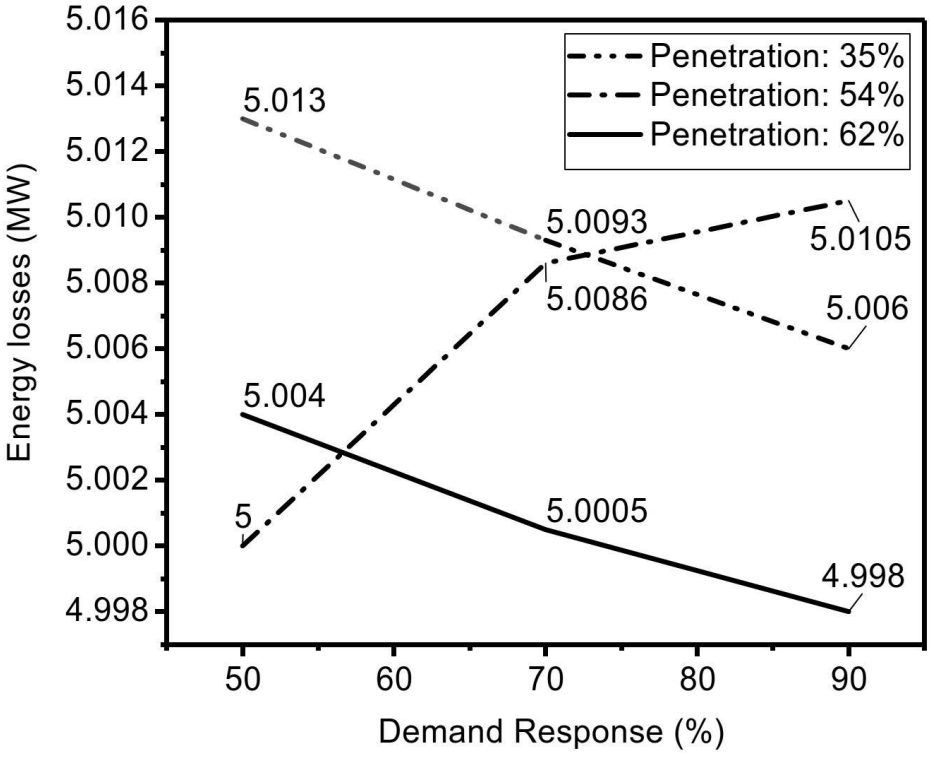

Figure 4.15: Case-II Energy losses.

4.5.3 Case-III: Effect of PHEV with DGs

This case represents the system with three penetration levels of PHEV, and DGs with the conventional load. Dispatchable DGs are considered according to their availability, capacity and cost as given in Appendix II. The load demands are fulfilled by CPG, DGs and by discharging of EVs.

The overall load (residential, commercial and industrial) patterns and reduced load demands due to DGs are shown in Fig 4.16. It is observed that the peak load occurs at 12 : 00 hour. The scheduling of DGs reduces peak load demand on distribution network by 0.0568 p.u. The hourly scheduling of DGs is shown in Fig. 4.17. The comparison of hourly minimum system voltage for Case-II and Case-III at 62% penetration level of PHEV is shown in Fig 4.18. It is observed that the hourly minimum system voltage profile significantly improves after optimal scheduling of the DGs.

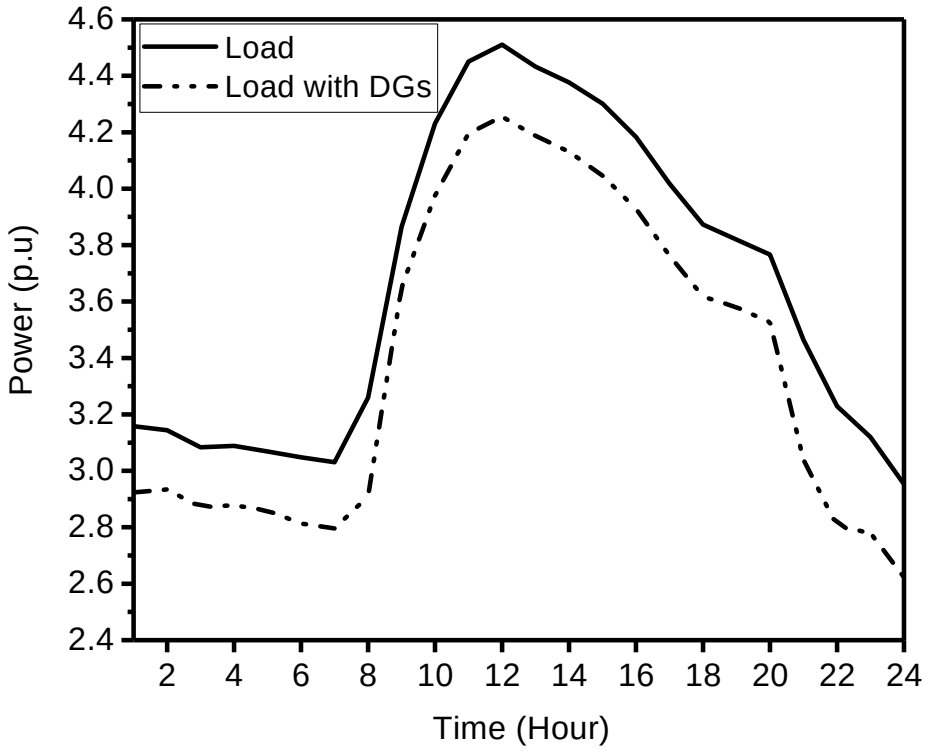

Figure 4.16: Overall load pattern and reduced load demands due to DGs

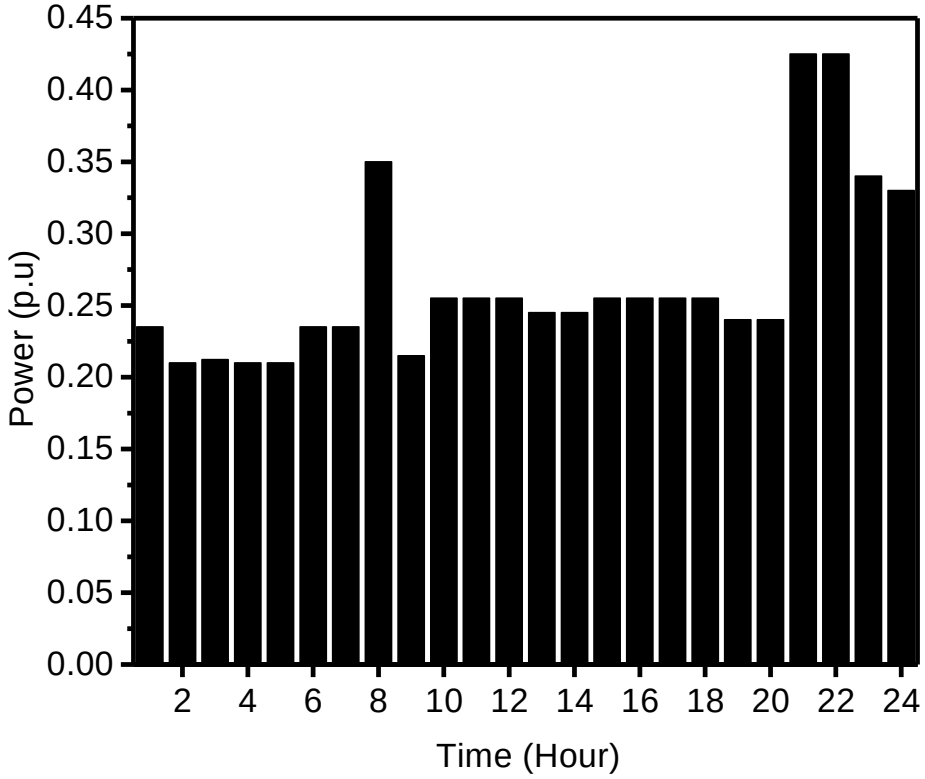

Figure 4.17: Total scheduled power of DGs.

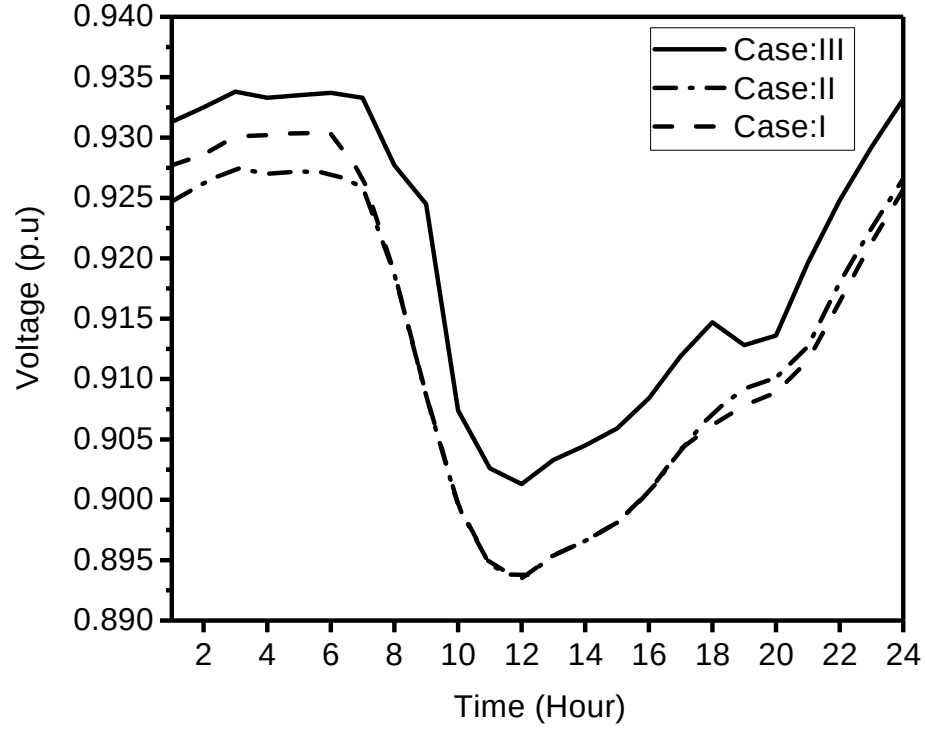

Figure 4.18: Comparison of hourly system minimum voltages at 62% PHEV penetration.

As far as system voltage profile is concerned in Case-I and Case-II, regardless of penetration level, it is observed that there is no improvement in the minimum voltage level during 12 : 00 hour for Case-II but in Case-III it is improved. This is due to scheduling of DGs during these hours. However, as depicted in Fig 4.18 the voltage levels during G2V mode (01 : 00 -06 : 00 hour) and V2G mode (18 : 00 - 24 : 00 hour) are also improved. It is also observed that the minimum voltage is lower in case of G2V (01 : 00 - 06 : 00 hour) period but in period of V2G is higher as the DR increases. Fig. 4.19 shows comparison of hourly voltage based on demand response at 62% level of penetration of vehicles.

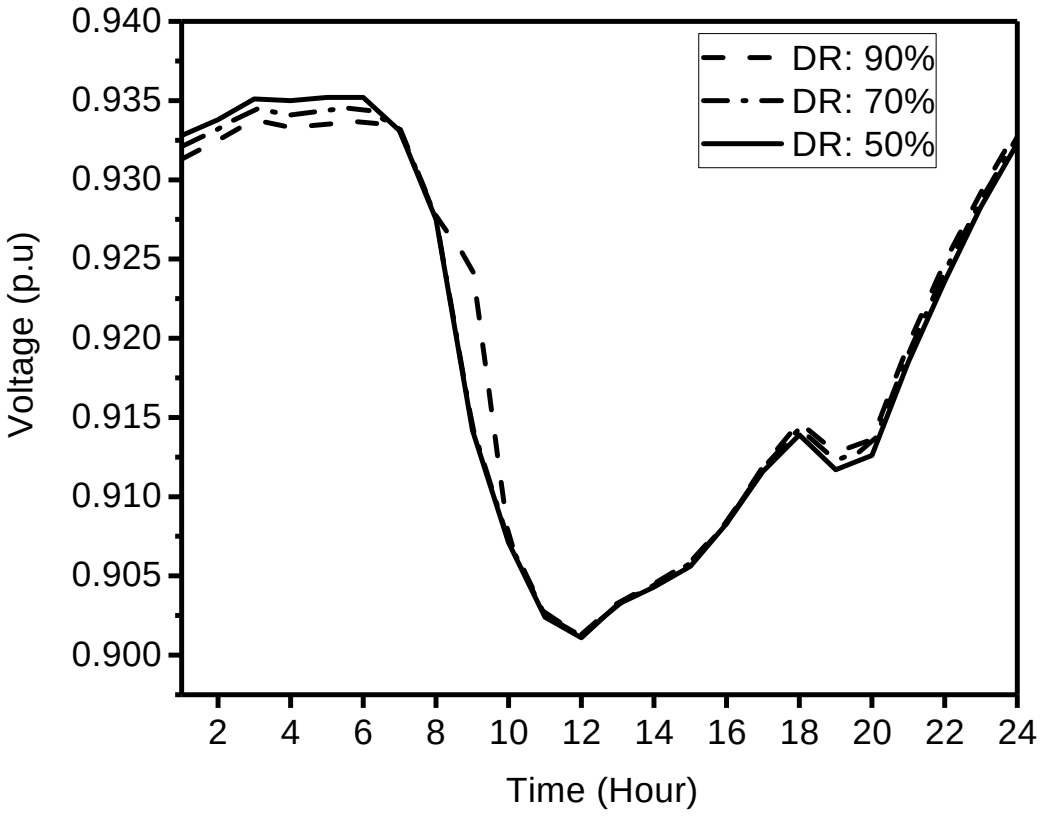

Figure 4.19: Case-III Comparison of voltage based on DR at 62% penetration level.

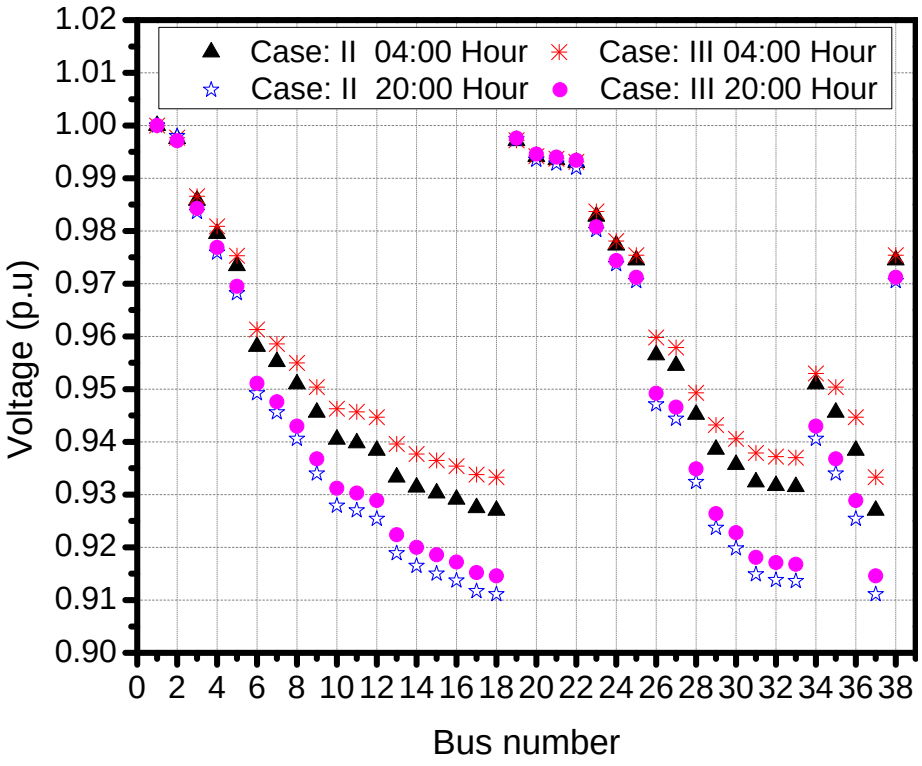

Figure 4.20: Comparison of bus wise voltage profile at 62% penetration levels and 90% DR

The comparison of bus-wise system voltage profiles for 04 : 00 hour (Valley hours) and 20 : 00 hour (peak hours) at 62% penetration level for Case-II and Case-III is shown in Fig 4.20. It is observed that at both periods bus-wise voltage profile get improved in Case-III i.e when DGs are scheduled.

The hourly optimal value of each objective function is depicted in Table 4.2 and the optimal hourly scheduling of individual DGs is presented in Fig. 4.21. The hourly energy losses at different penetration levels and at different DR levels are shown in Fig. 4.22. This figure shows comparison of energy losses for Case-I, Case-II and Case-III. It is observed that the in Case-II energy loss is higher as compare to Case-I (Base Case) and overall total energy loss is lower when system is incorporated with DGs.

Table 4.2: Outcomes of each objective function at 62% penetration level and 90% Demand response

Time (Hour)	f_1	f_2	f_3	F	Time (Hour)	f_1	f_2	f_3	F
1	0.2427	0.1296	0.2946	0.0526	13	0.4256	0.2684	0.4216	0.1534
2	0.2078	0.1262	0.2898	0.0425	14	0.4204	0.2613	0.4162	0.1491
3	0.2042	0.1204	0.2832	0.0407	15	0.4577	0.534	0.4099	0.1669
4	0.2045	0.1207	0.2844	0.0409	16	0.4459	0.2393	0.3989	0.1575
5	0.2034	0.1194	0.2832	0.0404	17	0.5097	0.2198	0.3836	0.1900
6	0.2351	0.1183	0.2823	0.0486	18	0.5379	0.2052	0.3708	0.2047
7	0.2338	0.121	0.2844	0.0486	19	0.6060	0.2053	0.374	0.2519
8	0.2934	0.1463	0.3122	0.0716	20	0.6367	0.2002	0.37	0.2738
9	0.3691	0.2029	0.3694	0.1125	21	0.6038	0.1769	0.3457	0.2445
10	0.4506	0.2449	0.4033	0.1612	22	0.5363	0.1547	0.3229	0.1942
11	0.4727	0.2715	0.4242	0.1795	23	0.4426	0.1381	0.3039	0.1361
12	0.4787	0.2793	0.43	0.1847	24	0.3290	0.1236	0.2867	0.0811

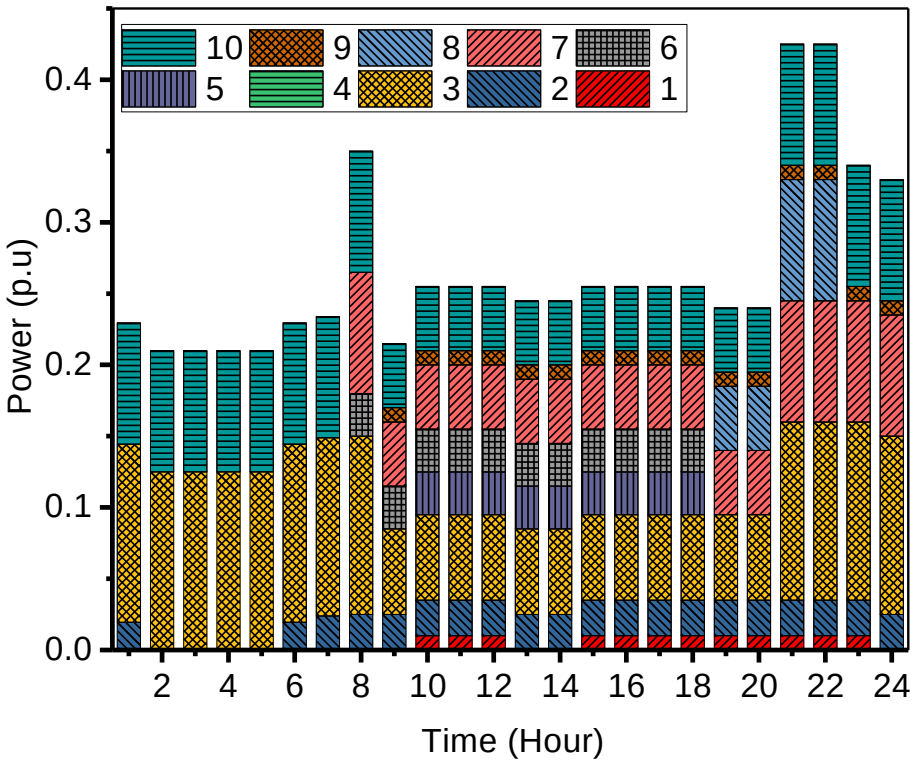

Figure 4.21: Hourly scheduled power of DGs (Legends show the DGs indices)

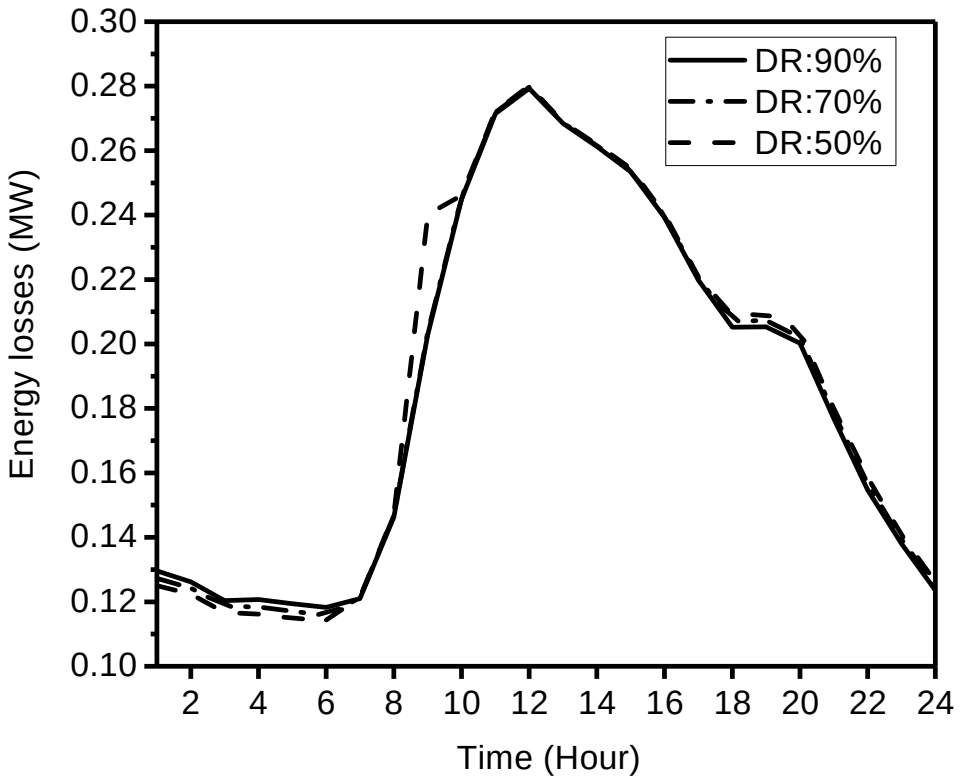

Figure 4.22: Comparison of energy losses at 90% DR

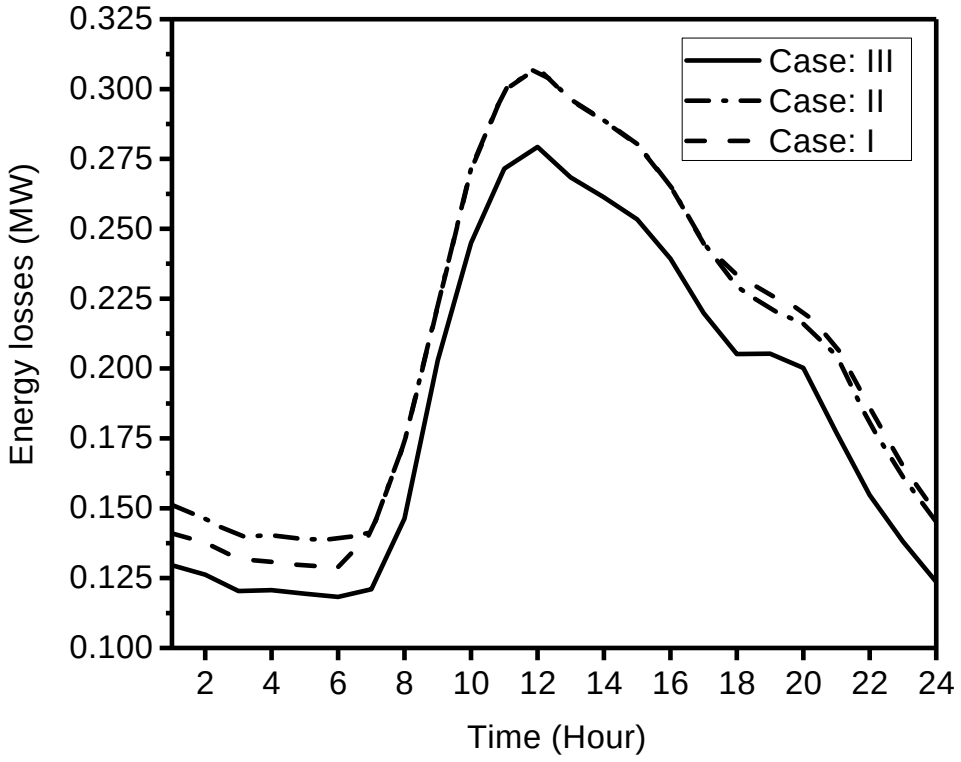

Figure 4.23: Comparison of energy losses based on DR at 62% penetration level

Fig. 4.23 shows the comparison of energy losses at 62% PHEV penetration at different DR levels. It is observed that the energy loss is higher as the DR increases in period of G2V (01 : 00 - 06 : 00) hour but in period of V2G it goes lower. As the overall total energy losses decreases as DR increases from 50% to 90%.

The outcomes of the Case-III are summarised in Figs. 4.24 & 4.25. Fig. 4.24 shows the characteristics of system cost versus DR for different penetration levels. In the present scenario, it is observed that the operating cost consistently lowers with increasing DR for each PHEV penetration level. The operating cost shows quite consistent effects with respect to DR.

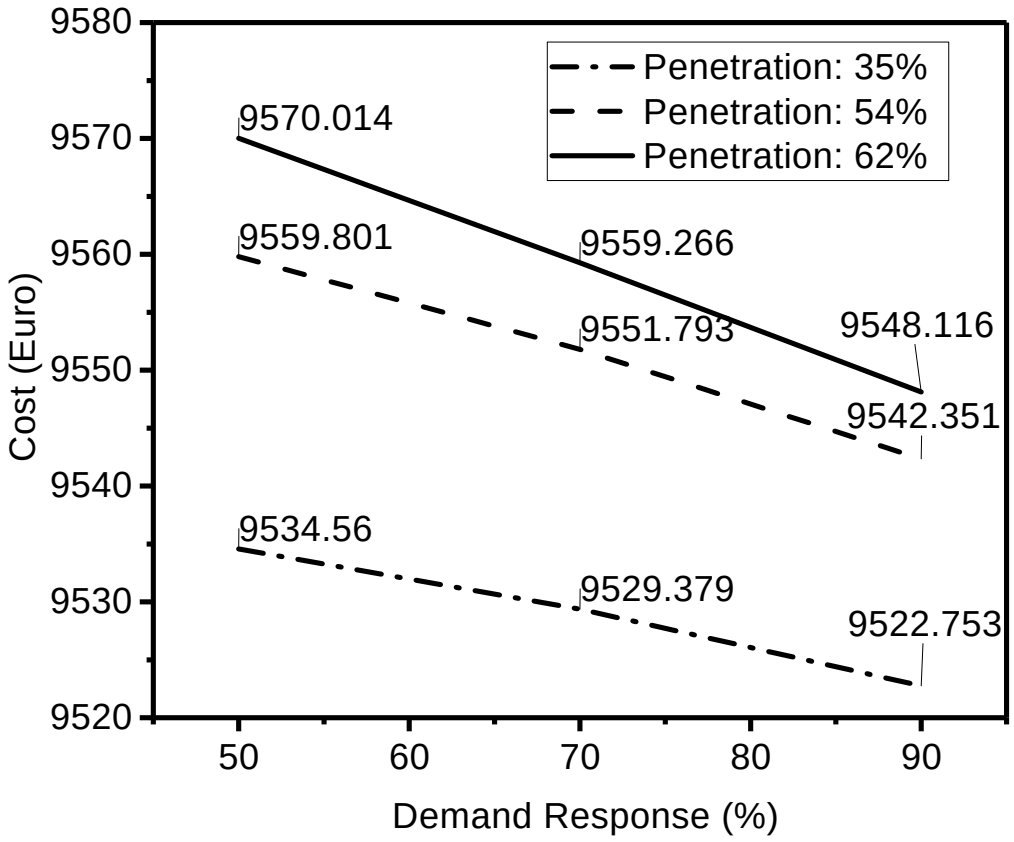

Figure 4.24: Case-III System cost

Fig. 4.25 shows the characteristics of energy losses versus DR for different penetration levels. In case of energy losses, it is observed that for penetration level of 62% and at DR of 50% the energy loss is higher then penetration level of 54% at same DR. However, at other levels of DR, the losses consistently lowers with penetration level. The energy losses show quite consistent effects with respect to penetration levels.

If we compare the results obtained in Case-III with case-II, system cost and energy

losses both are reduced. Basically, the optimal scheduling governs coordination of DGs in conjunction with CPG and PHEV. After, scheduling the DGs output in optimal manner, reduced system cost, reduced energy losses and improved voltage profile are observed.

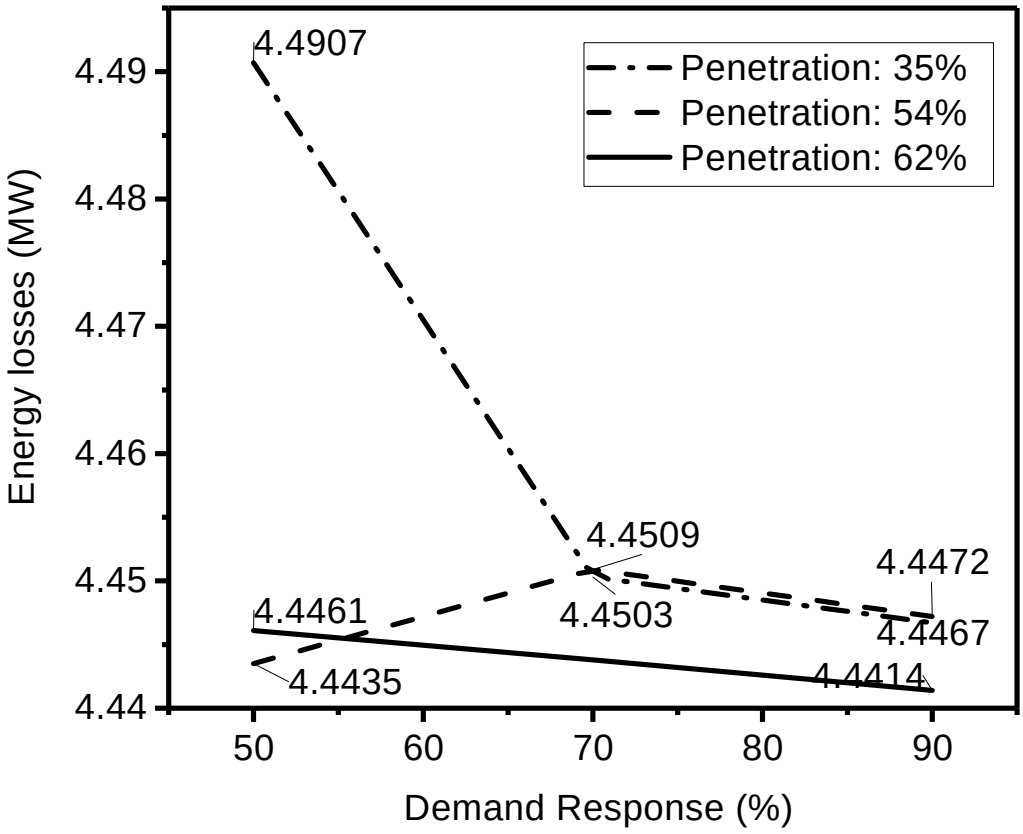

Figure 4.25: Case-III Energy losses

4.6 Summary

In this chapter, a 24-hour scheduling of DGs coordinated with G2V and V2G connection of PHEV has been proposed. The problem is formulated as non-linear, mixed integer and non-convex optimization problem. The resulting optimization problem is solved using DE. It is observed that the system cost is significantly impacted by the demand responsiveness and penetration levels of PHEV. It is observed that introduction of effective DR programme and optimal DG scheduling can reduced the system operating cost even at higher penetration level. The system losses decrease when the DGs are scheduled in the system. The flattening of load curve and voltage profile improvement is observed when the DGs are scheduled optimally. The outcomes of planning algorithm are, reduction in

system losses and improvement in voltage profile by DGs scheduling. It is observed that the proposed idea is useful for accommodating high penetration of electric vehicle in future for higher demand responsive system. Thus, when PHEVs are introduced, performance characteristics of distribution system deteriorate. These performance characteristics cannot be improved without proper scheduling of distributed resources. Hence, improvement in characteristics by scheduling DGs has been studied and it has been demonstrated that system operating cost, losses, voltage profile and load flattening improved with the proposed method scheduling of DGs and PHEVs.